Open Access Full Text Article

ORIGINAL RESEARCH

Enhanced primary tumor delineation in pancreatic adenocarcinoma using ultrasmall super paramagnetic iron oxide nanoparticle-ferumoxytol: an initial experience with histopathologic correlation

Sandeep S Hedgire[1]
Mari Mino-Kenudson[2]
Azadeh Elmi[1]
Sarah Thayer[3]
Carlos Fernandez-del Castillo[3]
Mukesh G Harisinghani[1]

[1]Department of Abdominal Imaging and Intervention, [2]Department of Pathology, [3]Department of Surgery, Massachusetts General Hospital, Boston, MA, USA

Purpose: To evaluate the role of ferumoxytol-enhanced magnetic resonance imaging (MRI) in delineating primary pancreatic tumors in patients undergoing preoperative neoadjuvant therapy.

Materials and methods: Eight patients with pancreatic adenocarcinoma were enrolled in this study, and underwent MRI scans at baseline, immediate post, and at the 48 hour time point after ferumoxytol injection with quantitative T2* sequences. The patients were categorized into two groups; group A received preoperative neoadjuvant therapy and group B did not. The T2* of the primary pancreatic tumor and adjacent parenchyma was recorded at baseline and the 48 hour time point. After surgery, the primary tumors were assessed histopathologically for fibrosis and inflammation.

Results: The mean T2* of the primary tumor and adjacent parenchyma at 48 hours in group A were 22.11 ms and 16.34 ms, respectively; in group B, these values were 23.96 ms and 23.26 ms, respectively. The T2* difference between the tumor and adjacent parenchyma in group A was more pronounced compared to in group B. The tumor margins were subjectively more distinct in group A compared to group B. Histopathologic evaluation showed a rim of dense fibrosis with atrophic acini at the periphery of the lesion in group A. Conversely, intact tumor cells/glands were present at the periphery of the tumor in group B.

Conclusion: Ferumoxytol-enhanced MRI scans in patients receiving preoperative neoadjuvant therapy may offer enhanced primary tumor delineation, contributing towards achieving disease-free margin at the time of surgery, and thus improving the prognosis of pancreatic carcinomas.

Keywords: pancreatic cancer, tumor margin, neoadjuvant therapy, borderline resectable pancreatic cancer

Introduction

Pancreatic cancer is the fourth leading cause of cancer-related death in the US, with an overall 5-year survival rate of 5%.[1] Even localized disease has a 5-year survival rate of only 18%–24%.[2] According to the American Cancer Society's estimates, 45,220 pancreatic cancers will be diagnosed in 2013 and 38,460 patients will die of pancreatic cancer.[3] In spite of significant improvements in operative techniques and postoperative mortality rates, the overall survival for these patients has not changed significantly

Correspondence: Sandeep S Hedgire
Department of Abdominal Imaging and Intervention, Massachusetts General Hospital, 55 Fruit St, Boston, MA, USA
Tel +1 617 724 4266
Fax +1 617 726 4891
Email hedgire.sandeep@mgh.harvard.edu

over the past four decades.[4] Borderline resectable pancreatic cancers exemplify a subset of locally advanced pancreatic cancer (LAPC). Up to 30% of patients present with LAPC.[5] National Comprehensive Cancer Network (NCCN) guidelines v2.2012[6] have laid out the criteria for borderline resectable pancreatic tumor. The guidelines clearly emphasize the need to delineating the tumor from superior mesenteric vein (SMV), portal vein, gastrodudenal artery, hepatic artery and superior mesenteric artery (SMA). The guidelines also highlighted characterizing the involvement of these vessels in terms of impingement, abutment, narrowing, occlusion and encasement. The tumor is considered to be borderline resectable if it fulfills these criteria and shows no evidence of distant metastasis.[6] This category carries higher risk of margin-positive resection.

Currently, preoperative neoadjuvant therapy is often used for patients with borderline resectable tumors.[7] Anatomic staging is performed both before and after chemotherapy and/or chemoradiation with the use of multidetector computed tomography (CT). With such therapy, a large number of cancer cells are destroyed and thereafter replaced by fibrosis.[7] In the pancreas, the acinar epithelium is more sensitive to radiation compared to the islet cells and post-radiation therapy appearance may simulate pancreatitis.[8,9] The post-treatment response is usually seen as soft tissue on restaging CT scan, leaving the nature of this soft tissue open to speculation of post-neoadjuvant morphologic change or tumor progression. Moreover, because of the overlapping soft tissue attenuation, CT can not reliably distinguish between the two.[10] This soft tissue often tends to make the tumor margin indistinct, posing an additional challenge to the operating surgeon who aims for achieving disease-free margin. Thus, there is a need for a non-invasive imaging tool that allows the accurate delineation of treatment response from an adjacent viable tumor.[10,11]

Conventional magnetic resonance imaging (MRI) with gadolinium depicts enhancement patterns and provides no information at the cellular level. Ferumoxytol, by virtue of its cellular uptake, is more relevant than conventional MRI, which cannot provide information on the tumor margin of aggressive tumors like pancreatic carcinoma.

With this background, we sought to evaluate the role of ferumoxytol-enhanced MRI in delineating primary tumors in pancreatic adenocarcinoma patients undergoing preoperative neoadjuvant therapy. The objective of our study was to investigate if "functional" imaging with ferumoxytol can provide more precise tumor margin delineation than conventional

"structural" imaging in patients undergoing neoadjuvant therapy for pancreatic carcinoma.

Materials and methods
Patient population
In this institutional review board approved, Health Insurance Portability and Accountability Act (HIPPA) compliant study, ten patients with biopsy-proven pancreatic adenocarcinoma were included initially. These patients were drawn from a larger prospective study aimed at the detection of lymph node metastasis following the administration of ultrasmall superparamagnetic iron oxide particles (USPIO ferumoxytol). These patients were screened for the inclusion criteria of locally resectable or borderline resectable pancreatic carcinoma and underwent the MRI scans after signing the written informed consent form. Patients with unresectable disease (and/or distant metastasis at the time of initial screening), those who didn't undergo surgery even after undergoing study procedure, and those who had contraindications for undergoing MRI (metallic foreign body/pacemaker/claustrophobia) were excluded. Pregnant women and patients predisposed to iron overload (secondary to conditions like thalassemia) were also excluded.

The patients were categorized into two distinct groups; A) those with borderline resectable tumor who received preoperative neoadjuvant therapy (with 25 Gy of proton beam radiation and concurrent capecitabine) and B) those with resectable tumor who did not receive preoperative neoadjuvant therapy. The patients in group A had borderline resectable tumor and underwent preoperative neoadjuvant therapy that was aimed at downstaging the tumor to resectable status.

Characteristics and administration of the contrast agent
Ferumoxytol (AMAG Pharmaceuticals, Lexington, MA, USA) is an USPIO nanoparticle with an average colloidal particle size of 30 nm by light scattering and a molecular weight of 750 kDa. It is comprised of a nonstoichiometric magnetite core covered by a semisynthetic carbohydrate coating of polyglucose sorbitol carboxymethylether designed to minimize immunological sensitivity. Ferumoxytol is available as a sterile, neutral pH liquid containing 30 mg of elemental iron per mL. The blood half-life is dose dependent and is approximately 14.5 hours at a dose of 4 mg/kg. All patients received ferumoxytol intravenously at a dose of 6 mg/kg of body weight to a maximum dose of 510 mg (17 mL)

of elemental iron. Ferumoxytol was administered by hand injection at the rate of 1 mL/second, which was chased by a saline bolus of 10 mL. Each patient was monitored for the development of adverse effects of ferumoxytol.

MRI and analysis

MRI of the upper abdomen (T1, T2, and T2*-weighted imaging) was performed on a 3T system (Magnetom Trio, A Tim System; Siemens, Erlangen, Germany) using an 8-channel phased array body coil, before, immediately after, and 48 hours after the intravenous administration of ferumoxytol. Considering the pharmacokinetics of ferumoxytol, we chose to scan the patients at 48 hours post-ferumoxytol administration to allow its accumulation in the tissues. Imaging duration ranged from 30 to 45 minutes. Quantitative T2* sequences were performed as breath-hold, mono-polar, multi-echo, gradient echo sequences with six in-phase, equally spaced echoes (TE =2.5–14.8, TR =169 ms, thickness =4 mm) in all patients.

Group A patients underwent MRI scans after completing the preoperative neoadjuvant therapy and before the scheduled Whipple's surgery. Group B patients underwent MRI scans before their scheduled Whipple's surgery. The MRI images were loaded onto the OsiriX DICOM viewer (http://www.osirix-viewer.com; 64-bit version ©Pixmeo SARL) for image viewing and post-processing. These scans were reviewed by two radiologists (with 5 and 20 years of experience in reading abdominal MRI scans, respectively) and the T2 value* of primary tumor and adjacent disease-free parenchyma at the 48 hour time point were measured as consensus by drawing equal sized, non-overlapping, oval-shaped, operator-dependent regions of interest (ROI).

Based on the contiguity of pancreatic parenchyma and following the pancreatic duct, the pancreatic parenchyma in the vicinity of the tumor was chosen depending on its differential signal characteristics on T1- and T2-weighted images. The difference between the two values (ΔT2*) was calculated for both groups. The tumor margin was subjectively assessed. Conspicuity of the tumor margin on the conventional T1- and T2-weighted images both pre- and post-ferumoxytol was compared to the T2*-weighted images on post-ferumoxytol injection scan at the 48 hour time point in all ten patients as consensus on a 4-point scale: 1) distinct margin; 2) perceptible margin; 3) mixed margin (partly perceptible, partly imperceptible); and 4) imperceptible margin.

The interface between the tumor and SMV portal vein, gastroduodenal artery, and SMA was also assessed subjectively. The length of time between the scan date and date of surgery was recorded for all patients. The length of time between the last day of neoadjuvant therapy and surgery was recorded for group A.

Histopathologic analysis

After the Whipple's procedure, the resected surgical specimens were fixed in 10% neutral buffered formalin, embedded in paraffin, sectioned, and stained with hematoxylin-eosin (HE). Two patients who did not undergo Whipple's procedure were excluded. Histopathologic analysis was performed by a gastrointestinal (GI) pathologist specialized in the field with over 10 years of experience. The tumor margins (transection, uncinate, and posterior) were assessed along with the tumor/fibrosis ratio.

Results

Of the eight patients, four each were part of group A and group B. Each group comprised two women and two men. The average age was 68.6 years in group A and 70.8 years in group B. No adverse events were noted following ferumoxytol injection. All images were considered of diagnostic quality. The average area of the region of interest (ROI) was 0.5 cm². The mean T2* of the tumor and adjacent parenchyma at 48 hours in group A were 22.11 ms (SD: 12.3) and 16.34 (SD: 2.3) ms, respectively. In group B, these values were 23.96 ms for the tumor (SD: 10.6) and 23.26 ms for the adjacent parenchyma (SD: 8.5). While T2* values of the tumor did not differ greatly, the T2* values of the adjacent parenchyma between the two groups were strikingly different. The T2* difference (ΔT2*) between the tumor and adjacent parenchyma in patients who received neoadjuvant therapy was more pronounced compared to the difference in patients who did not receive neoadjuvant therapy (5.77 ms in group A [SD: 9.5] vs 0.70 ms in group B [SD: 7]; Figure 1).

The tumor margins were subjectively more distinct in group A compared to perceptible margins in group B. The margins were better appreciated on the T2*-weighted images compared to the conventional T1- or T2-weighted images. Even in the group A patients, the margins were better delineated on post-ferumoxytol–enhanced scans at the 48 hour time point compared to the baseline scan. The interface between the tumor and SMV portal vein, gastroduodenal artery, and SMA was clearly identified by both reviewers (Figure 2). The mean duration between the scan and surgery was 7.3 days and the mean duration between
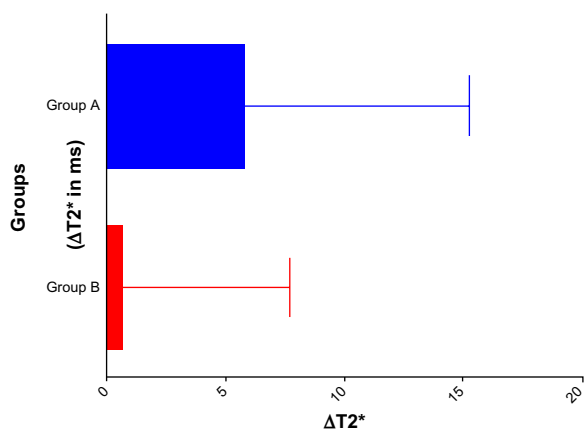
Figure 1 Graph showing ΔT2* (difference between the T2* value of the tumor and adjacent parenchyma) in group A and B.
**Note:** Whiskers represent standard error of the mean.

the last day of neoadjuvant therapy and surgery in group A was 18 days.

Histopathologic evaluation showed prominent fibrosis with scattered residual tumor glands within the lesion (therapeutic effect) resulting in a low tumor/fibrosis ratio, and a rim of dense fibrosis around the tumor (that is, well demarcated from the intact parenchyma at its periphery) in group A. Conversely, the majority of the lesion consisted of intact tumor cells/glands, and the tumor/fibrosis ratio was
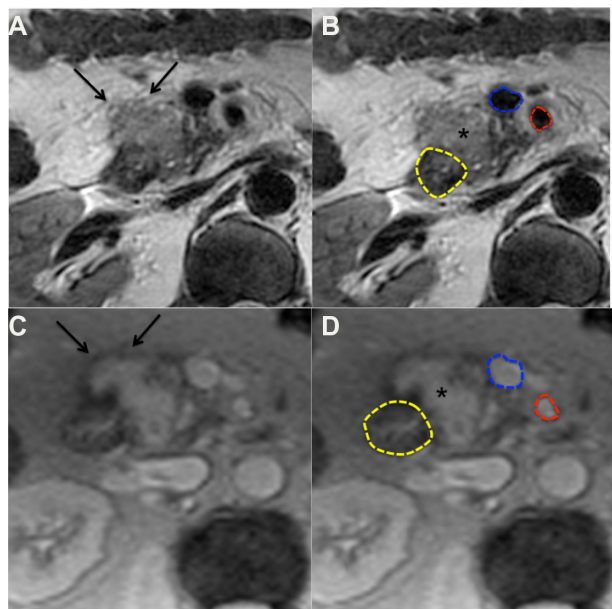
Figure 2 T2- (**A** and **B**) and T2*- (**C** and **D**) weighted images of a 55-year-old man showing pathologically proven pancreatic adenocarcinoma arising from the pancreatic head (asterisk in **B** and **D**).
Notes: More distinct tumor margins (arrows) are visible on the T2*-weighted image (**C**) compared to conventional T2 weighted image (arrows in **A**). The interface between the duodenal lumen (yellow in **B** and **D**), superior mesenteric vein (blue in **B** and **D**), and superior mesenteric artery (red in **B** and **D**) is also more clearly depicted on T2*-weighted images (**C** and **D**) compared to the conventional T2 images (**A** and **B**).
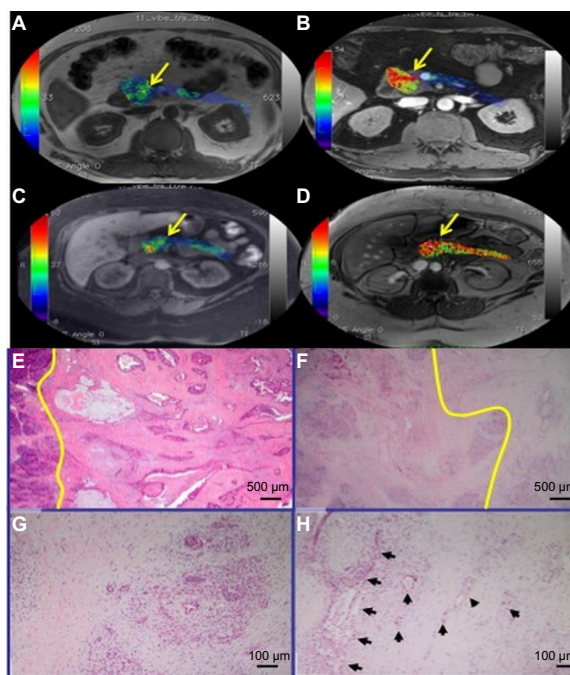
Figure 3 Pseudofused images of T2* maps over T1-VIBE pre- and post-ferumoxytol (**A**) and (**B**) showing distinct tumor margin (arrow) in a 55-year-old man who underwent neoadjuvant therapy. Pseudofused images of T2* maps over T1-VIBE pre- and post-ferumoxytol (**C** and **D**) showing less distinct tumor margin (arrow) in a 62-year-old man who did not undergo neoadjuvant therapy. (**E**) non-neoadjuvant; (**F–H**) neoadjuvant cases: yellow lines indicate a boundary between non-neoplastic parenchyma (left) and the tumor; (**G**) atrophic acini in the background of dense fibrosis; (**H**) several malignant glands (arrows) with therapeutic effects are seen in a patchy distribution in the background of dense fibrosis. Of note, the rim of the fibrotic non-neoplastic parenchyma is well demarcated from the intact pancreatic tissue at its periphery.
Notes: (**E**) and (**F**) at 20× magnification; (**G–H**) at 100× magnification.

significantly higher in group B (Figure 3). The tumor margins were disease free in all eight patients. Two patients (one in each group) did not undergo Whipple's procedure due to hepatic metastasis detected on preoperative imaging.

Discussion

Strategies to improve the prognosis of pancreatic cancer are constantly evolving.[12] A well-performed pancreatic protocol CT is a popular approach in staging pancreatic cancer and has been validated well in the literature.[13–15] MRI has also been proved equally efficacious in predicting vascular and nodal involvement.[16,17] CT, however, has limited capacity to characterize the nature of post-radiation soft tissue attenuation.[10] In fact, Katz et al, in their study of 129 patients with borderline resectable pancreatic carcinoma, concluded that radiographic downstaging was a rarity following neoadjuvant therapy.[18] One of the reasons for the inaccurate delineation of the tumor margin is ill-defined boundaries, which is typical for pancreatic cancer, causing difficulty in identifying the full volume of the tumor mass.[19] Sohn et al showed that there is

a >50% increase in 5-year mortality following a margin-positive resection.[20] The significance of margin-negative resection was also studied by Howard et al, who reported a similar outcome, where the 5-year mortality was 39% higher in patients with a margin-positive resection compared to those with negative margins.[21] Thus, it is not surprising that it is the main cause of local disease recurrence and grim prognosis.[20] Hence, there is a need to develop alternative imaging methods in this regard.

Iron oxide-based USPIOs have been widely used for the characterization of nodal metastasis in various abdomino-pelvic malignancies.[22,23] Ferumoxytol is a newer USPIO, which is FDA-approved for the treatment of iron deficiency anemia in patients with chronic renal disease and has also been utilized to image inflammation in animal studies.[24–26] Another super paramagnetic iron oxide-ferucarbotran was recently studied by Kakite et al in animal models to evaluate ablated liver parenchyma.[27] This observation was further validated in human studies, which demonstrated the use of impaired clearance of ferucarbotran to assess ablative margin and predict residual or recurrent tumor in patients undergoing radiofrequency ablation for hepatocellular carcinoma.[28,29] Ferumoxytol has been used for tumor imaging before by Muldoon et al for intracerebral tumors in animal models. They assessed the antiangiogenic response of chemotherapeutic agents with the use of ferumoxytol.[30] The utility of iron oxide nanoparticles selectively targeting mammary cancer cells for the detection of micrometastasis was recently demonstrated in vivo and in vitro in a study by Kievit et al.[31] However, to the best of our knowledge, USPIOs have not been used for the delineation of the tumor margin in pancreatic carcinomas. We observed the T2* gradient between the tumor and adjacent disease-free parenchyma in our study, with higher T2* values in the tumor and lower values in adjacent parenchyma in group A. Considering the neoadjuvant therapy directed at the tumor site, the inflammatory response triggered by neoadjuvant therapy explains the higher T2* values, conveying a higher amount of intracellular ferumoxytol in the tumor region compared to the adjacent parenchyma and subsequent lower tumor-to-fibrosis ratio on histopathologic analysis. As this driving force in the form of neoadjuvant therapy was not present in group B, this group did not have the same degree of inflammation sequel and iron accumulation, thereby showing a narrow gradient in T2* and a higher tumor/fibrosis ratio. The remarkable difference in the T2* of adjacent parenchyma between the two groups can also be attributed to the neoadjuvant therapy, as such therapy also affects normal pancreatic cells, leading to cyanosis secondary to impairment of blood flow.[32]

This apparent T2* gradient seen in our study may be used for better tumor delineation of the pancreatic cancer, thereby affecting surgical planning. The delineation of the tumor margin was better in patients with preoperative neoadjuvant therapy (Group A) in our study. T2*-weighted images acquired 48 hours after ferumoxytol injection can offer an added advantage over the conventional T2-weighted image. This is supported by our observation of enhanced tumor margin delineation on the T2*-weighted post-ferumoxytol scan at the 48 hour time point in comparison with conventional T1- and T2-weighted images, even in group A.

Our study is limited by the small sample size and the fewer number of patients who underwent preoperative neoadjuvant therapy. We could not analyze the primary tumor on histopathology in two patients. We also restricted our sample size to resectable/borderline resectable pancreatic cancer patients. We assessed the tumor to fibrosis ratio subjectively and did not quantify iron accumulation histopathologically using special stains. However, we hope to highlight a potential application of ferumoxytol-enhanced MRI in enhanced delineation of pancreatic primary tumor margin with our preliminary data and to warrant the development of ferumoxytol-enhanced MRI as a diagnostic tool for pancreatic cancer. This observation can also be used to predict the status of the tumor margin on histopathology in future studies. Additionally, this observation may be applied to image other primary tumors following neoadjuvant therapy.

To conclude, by better delineation of pancreatic cancer on ferumoxytol-enhanced MRI scans in patients receiving preoperative neoadjuvant therapy, imaging may contribute a roadmap for the surgeons and can aid in achieving disease-free margin at the time of surgery, thus improving the prognosis of pancreatic carcinoma.

Author contributions

Acknowledgment

Disclosure

The authors report no conflicts of interest in this work.

References

1. Saif MW. Advancements in the management of pancreatic cancer: 2013. *JOP J Pancreas*. 2013;14(2):112–118.
2. Yeo CJ, Abrams RA, Grochow LB, et al. Pancreaticoduodenectomy for pancreatic adenocarcinoma: postoperative adjuvant chemoradiation improves survival. A prospective, single-institution experience. *Ann Surg*. 1997;225(5):621–633; discussion 633–636.
3. American Cancer Society. *Cancer Facts and Figures 2013*. Atlanta: American Cancer Society; 2013. Available at: http://www.cancer.org/cancer/pancreaticcancer/detailedguide/pancreatic-cancer-key-statistics. Accessed February 18, 2014.
4. Garcea G, Dennison AR, Pattenden CJ, Neal CP, Sutton CD, Berry DP. Survival following curative resection for pancreatic ductal adenocarcinoma. A systematic review of the literature. *JOP J Pancreas*. 2008;9(2):99–132.
5. Hidalgo M. Pancreatic cancer. *N Engl J Med*. 2010;362(17):1605–1617.
6. Tempero MA, Arnoletti JP, Behrman SW, et al. Pancreatic Adenocarcinoma, version 2.2012: featured updates to the NCCN Guidelines. *J Natl Compr Cancer Netw JNCCN*. 2012;10(6):703–713.
7. Cooper AB, Tzeng CW, Katz MH. Treatment of borderline resectable pancreatic cancer. *Curr Treat Options Oncol*. 2013;14(3):293–310.
8. Iyer R. Radiation injury: imaging findings in the chest, abdomen and pelvis after therapeutic radiation. *Cancer Imaging*. 2006;6:S131–S139.
9. Lawrence TS, Robertson JM, Anscher MS, Jirtle RL, Ensminger WD, Fajardo LF. Hepatic toxicity resulting from cancer treatment. *Int J Radiat Oncol Biol Phys*. 1995;31(5):1237–1248.
10. Erkan M, Reiser-Erkan C, Michalski CW, et al. The impact of the activated stroma on pancreatic ductal adenocarcinoma biology and therapy resistance. *Curr Mol Med*. 2012;12(3):288–303.
11. De Gaetano AM, Rufini V, Castaldi P, et al. Clinical applications of (18)F-FDG PET in the management of hepatobiliary and pancreatic tumors. *Abdom Imaging*. 2012;37(6):983–1003.
12. Michl P, Gress TM. Current concepts and novel targets in advanced pancreatic cancer. *Gut*. 2013;62(2):317–326.
13. Callery MP, Chang KJ, Fishman EK, Talamonti MS, William Traverso L, Linehan DC. Pretreatment assessment of resectable and borderline resectable pancreatic cancer: expert consensus statement. *Ann Surg Oncol*. 2009;16(7):1727–1733.
14. Horton KM, Fishman EK. Adenocarcinoma of the pancreas: CT imaging. *Radiol Clin North Am*. 2002;40(6):1263–1272.
15. Klauss M, Schöbinger M, Wolf I, et al. Value of three-dimensional reconstructions in pancreatic carcinoma using multidetector CT: initial results. *World J Gastroenterol*. 2009;15(46):5827–5832.
16. Ichikawa T, Haradome H, Hachiya J, et al. Pancreatic ductal adenocarcinoma: preoperative assessment with helical CT versus dynamic MR imaging. *Radiology*. 1997;202(3):655–662.
17. Schima W, Ba-Ssalamah A, Goetzinger P, Scharitzer M, Koelblinger C. State-of-the-art magnetic resonance imaging of pancreatic cancer. *Top Magn Reson Imaging*. 2007;18(6):421–429.
18. Katz MHG, Fleming JB, Bhosale P, et al. Response of borderline resectable pancreatic cancer to neoadjuvant therapy is not reflected by radiographic indicators. *Cancer*. 2012;118(23):5749–5756.
19. Krishnamoorthy SK, Hayim M, Vestal T, Saif MW. Highlights on novel imaging methods of pancreatic cancer. *JOP J Pancreas*. 2013;14(4):388–390.
20. Sohn TA, Yeo CJ, Cameron JL, et al. Resected adenocarcinoma of the pancreas-616 patients: results, outcomes, and prognostic indicators. *J Gastrointest Surg Off J Soc Surg Aliment Tract*. 2000;4(6):567–579.
21. Howard TJ, Krug JE, Yu J, et al. A margin-negative R0 resection accomplished with minimal postoperative complications is the surgeon's contribution to long-term survival in pancreatic cancer. *J Gastrointest Surg Off J Soc Surg Aliment Tract*. 2006;10(10):1338–1345; discussion 1345–1346.
22. Harisinghani M, Ross RW, Guimaraes AR, Weissleder R. Utility of a new bolus-injectable nanoparticle for clinical cancer staging. *Neoplasia*. 2007;9(12):1160–1165.
23. Saokar A, Islam T, Jantsch M, Saksena MA, Hahn PF, Harisinghani MG. Detection of lymph nodes in pelvic malignancies with Computed Tomography and Magnetic Resonance Imaging. *Clin Imaging*. 2010;34(5):361–366.
24. Lu M, Cohen MH, Rieves D, Pazdur R. FDA report: Ferumoxytol for intravenous iron therapy in adult patients with chronic kidney disease. *Am J Hematol*. 2010;85(5):315–319.
25. Alam SR, Shah ASV, Richards J, et al. Ultrasmall superparamagnetic particles of iron oxide in patients with acute myocardial infarction: early clinical experience. *Circ Cardiovasc Imaging*. 2012;5(5):559–565.
26. Farrell BT, Hamilton BE, Dósa E, et al. Using iron oxide nanoparticles to diagnose CNS inflammatory diseases and PCNSL. *Neurology*. 2013;81(3):256–263.
27. Kakite S, Fujii S, Nakamatsu S, et al. Usefulness of administration of SPIO prior to RF ablation for evaluation of the therapeutic effect: an experimental study using miniature pigs. *Eur J Radiol*. 2011;78(2):282–286.
28. Koda M, Tokunaga S, Miyoshi K, et al. Assessment of ablative margin by unenhanced magnetic resonance imaging after radiofrequency ablation for hepatocellular carcinoma. *Eur J Radiol*. 2012;81(10):2730–2736.
29. Mori K, Fukuda K, Asaoka H, et al. Radiofrequency ablation of the liver: determination of ablative margin at MR imaging with impaired clearance of ferucarbotran – feasibility study. *Radiology*. 2009;251(2):557–565.
30. Muldoon LL, Gahramanov S, Li X, Marshall DJ, Kraemer DF, Neuwelt EA. Dynamic magnetic resonance imaging assessment of vascular targeting agent effects in rat intracerebral tumor models. *Neuro Oncol*. 2010;13(1):51–60.
31. Kievit FM, Stephen ZR, Veiseh O, et al. Targeting of primary breast cancers and metastases in a transgenic mouse model using rationally designed multifunctional SPIONs. *ACS Nano*. 2012;6(3):2591–2601.
32. Ryschich E, Schmidt J, Loeffler T, et al. Different radiogenic effects on microcirculation in healthy pancreas and in pancreatic carcinoma of the rat. *Ann Surg*. 2003;237(4):515–521.